Zhao et al. *Advances in Difference Equations* (2015) 2015:216
DOI 10.1186/s13662-015-0517-4

Advances in Difference Equations
a SpringerOpen Journal

RESEARCH Open Access

# The stable extrinsic extended finite element method for second order elliptic equation with interfaces

Jianping Zhao[1,2*], Yanren Hou[3], Lina Song[4] and Dongwei Gui[2]

*Correspondence:
zhaojianping@126.com
[1]College of Mathematics and System Sciences, Xinjiang University, Urumqi, 830046, China
[2]Cele National Station of Observation and Research for Desert-Grassland Ecosystem, Xinjiang Institute of Ecology and Geography, Urumqi, 830011, China
Full list of author information is available at the end of the article

**Abstract**

In this paper, a stable extrinsic extended finite element method (SXFEM) is proposed to solve the second order elliptic equation with discontinuous coefficients and interfaces. SXFEM is designed by the stable enrichment function and stress intensity factors (SIF)-type enrichment functions. It shows that the proposed SXFEM can get the optimal convergence order. Numerical experiments are presented to verify the feasibility of the new method for this type of problem and the superiority compared with the standard FEM and XFEM.

**Keywords:** extended finite element method; generalized finite element method; discontinuous coefficients; extrinsic; interface

## 1 Introduction

We consider the boundary value problem of the form

$$\begin{cases} -\nabla \cdot (a(x,y)\nabla u) = f(x,y), & (x,y) \in \Omega \backslash \Gamma, \\ u(x,y) = 0, & (x,y) \in \partial\Omega, \end{cases} \tag{1}$$

where $\Omega$ is a bounded domain in $\mathrm{R}^d$ $(d = 2, 3)$ with polygonal or polyhedral boundary $\partial\Omega$, $f \in L^2(\Omega), f \in L^2(\Omega)$, $\Gamma = \bigcup_i \Gamma_i$ is the internal interface that may consist of several pieces of local internal interfaces $\Gamma_i$, which are also called interfaces in what follows. Generally, any two different interfaces might be intersected, that is, $\Gamma_i \cap \Gamma_j \neq \emptyset$ $(i \neq j)$ is possible. The function $a(x,y) \in L^\infty(\Omega)$ satisfies

$$0 < \alpha \leq a(x,y) \leq \beta < \infty, \quad \forall (x,y) \in \Omega,$$

where $\alpha, \beta$ are constants. It assumes that the function $a(x,y)$ is discontinuous across the interface $\Gamma_i$ while it is continuous away from the interfaces. This interface problem appears in fluid dynamics and material science. The traditional finite difference method (FDM) and the finite element method (FEM) fail to solve such a problem due to the singularities of the interface. They need improvement to deal with such kind of interface problems. For the approximation of non-smooth solutions, there are two fundamentally different approaches. One approach of the improvement is to refine the discretization near the critical

regions. Remeshing is required in this case, *i.e.*, placing more grid-points along the interface and around the intersection. This strategy involves *a posteriori* error estimates. For example, Cai and Zhang [1] proposed recovery-based error estimators and Bernardi and Verfürth [2] proposed weighted-residual error estimators to deal with interface problems.

Another strategy of improvement is to enrich a polynomial approximation space so that the non-smooth solutions can be modeled independent of the mesh. For example, the immersed boundary method (IBM) [3] and the immersed interface method (IIM) [4] are developed based on finite difference, and they modify the standard centered difference approximation to maintain the second order accuracy [5–11] or to get higher order methods [12, 13], while the immersed finite element method (IFEM) developed in [14–18] is designed to cope with interface problem based on the finite element method (FEM). In this paper, we consider the complex interface problems such as interfaces intersecting with each other.

Meanwhile, a variety of modifications to the conventional FEM have been made within the framework of the partition of unity (PU). One typical example is the extended finite element method (XFEM). It was first realized by Belytschko and Black in [19] by enriching the nodes of the finite elements near the crack tips and along the crack surfaces with the asymptotic crack tip functions. Since then, such a method received wide publicity and quick progress [20–23]. During the same decades, the generalized finite element method (GFEM) based on the partition of unity method (PUM) [24–26] was widely used to solve various types of problems. All of these methods share the property that they add special enrichment functions to a standard approximation space.

Based on and inspired by the development of these methods in [26], we try to use XFEM for solving elliptic problems with interfaces. One of our goals is to make the condition number of the matrix for the discrete system comparable with FEM by extrinsic XFEM.

The rest of the paper is organized as follows. Section 2 introduces preliminary definition related to the XFEM and the weak form of (1). The main part of this paper is Section 3, in which the feasible stable XFEM and its error estimation are derived. The integration strategy for XFEM is discussed in Section 4, and some numerical experiments are presented in Section 5 to show the feasibility of the proposed algorithms. A final conclusion is drawn in Section 6.

## 2 Preliminary definitions

### 2.1 The weak form of the problem

We use the standard notation for the Sobolev space $H^k(\Omega) = W^{k,2}(\Omega)$ and its associated norm $\|\cdot\|_{H^k(\Omega)}$ and semi-norm $|\cdot|_{H^k(\Omega)}$, especially $H^0(\Omega) = L^2(\Omega)$. Then the weak formulation of (1) reads as follows: find $u \in H_0^1(\Omega)$ such that

$$B(u,v) := \int_\Omega a(x,y)\nabla u \cdot \nabla v \, dx\, dy = \int_\Omega fv \, dx\, dy = (f,v), \quad \forall v \in H_0^1(\Omega). \tag{2}$$

Since $a(x,y)$ is bounded and away from zero, the variational problem has a unique solution.

For convenience of later expression, for any subdomain $A \subseteq \Omega$, we introduce the following energy norm $\|v\|_{\varepsilon(A)}$:

$$\|v\|_{\varepsilon(A)}^2 = B_A(v,v), \quad \forall v \in H^1(A),$$

where $B_A(u,w) := \int_A a\nabla u \cdot \nabla w \, dx\, dy$ for any $u, w \in H^1(A)$.

### 2.2 The extrinsic XFEM

Let $\tau_h$ be a uniform rectangular mesh of the domain $\Omega$, and we define the mesh parameter $h > 0$, $\mathcal{N}$ is the set of nodes on the mesh $\tau_h$. Let $I := \{i \in \mathbb{Z}, 0 \le i \le N\}$, where $N = N(h)$ is an integer, which is the number of nodes in the mesh. For $i \in I$, let $\omega_i \subset \Omega$ be the impact area of $x_i$. Considering the Ritz-Galerkin implementation for the XFEM for a two-dimensional elliptic equation, finite-dimensional subspaces $V^h \subset H^1(\Omega)$, $V_0^h \subset H_0^1(\Omega)$ are used as the approximating trial and test spaces. The trial functions are

$$\mathbf{u}^h = \sum_{i\in I} N_i \mathbf{u}_i + \sum_{i\in I^{\mathrm{en}}} N_i \sum_j \psi(\phi)\mathbf{v}_j^i = \sum_{i\in I} N_i \Bigg(\mathbf{u}_i + \sum_j \psi(\phi)\mathbf{v}_j^i\Bigg). \tag{3}$$

Here, $N_i$ are the finite-element shape functions, $\phi(\mathbf{x})$ is the level set function, $u_i$ is the numerical solution of real node $x_i$, and $v_j^i$ is the solution of virtual nodes located on $x_i$. They are the unknown coefficients of approximation. $I^{\mathrm{en}} = I^h$ means that we can enrich all nodes if needed.

## 3 Stable extrinsic extended finite element method and error estimation

In this section we give the stable extended finite element algorithm step by step and give the estimation for L2-error and energy-error.

### 3.1 The stable extrinsic XFEM

Subordinate to the cover $\{\omega_i\}_{i\in I^h}$, let $\{N_i\}$ be $C^0$-PU. We can also describe the function $u^h$ as an $n_i$-dimensional local approximating space $V_i^h$ on each patch $\omega_i$.

$$V_i = \operatorname{span}\{\varphi_j^i\}_{j=1}^{n_i}, \quad \varphi_j^i \in H^1(\omega_i) \text{ and } \varphi_1^i = 1.$$

Here, $n_i$ is a positive integer. If $n_i = 1$, in $\omega_i^h$ we just use a standard FEM basis function. In other cases the local area needs a special function in order to mimic the exact solution there. The PUM form about (3) is precisely by (2), with the finite-dimensional space $V^h$ given by

$$V^h = \sum_{i\in I^h} N_i V_i = \operatorname{span}\{N_i\varphi_j^i, 1 \le j \le n_i, i \in I^h\} := S_1 + S_2,$$

where

$$S_1 = \Bigg\{\xi : \xi = \sum_{i\in I^h} u_i N_i\Bigg\}, \qquad S_2 = \Bigg\{\xi : \xi = \sum_{i\in I^h}\sum_{j=2}^{n_i} v_j^i \varphi_j^i N_i\Bigg\}$$

and $u^{i,h}, v_j^i \in \mathbb{R}$. If $n_i = 1, \forall i \in I^h$, $V = S_1$ the method is referred to as the Galerkin method. If $n_i > 1$, for example, in 1D problem and suppose $V_i = \mathcal{P}^2(\omega_i)$, $V_i = \operatorname{span}\{1, (x - x_i), (x - x_i)^2\}$, so $\varphi_1^i = 1$, $\varphi_2^i = (x - x_i)$, $\varphi_3^i = (x - x_i)^2$. $S_1 = \operatorname{span}\{N_i\}$, $S_2 = \operatorname{span}\{N_i\varphi_2^i, N_i\varphi_3^i\}$. $S_2$ is referred to as enrichments and enrichment spaces.

The extrinsic XFEM discretization of (1) is as follows: find $u^h \in V^h$ such that

$$B\big(u^h, v^h\big) = \big(f, v^h\big), \quad \forall v^h \in V^h(\Omega). \tag{4}$$

Extended approximations use locally enriched nodes with the aim to capture discontinuities and/or high gradients, and the linear dependencies are less frequently observed and often identified easily. At last the approximations of the form (3) do not have the Kronecker-$\delta$ property. Consequently, $u^h(x_i) \neq u_i$ makes the imposition of essential boundary conditions difficult.

Based on these problems, it is important to make (3) satisfy the Kronecker-$\delta$ property and linear independence. Babuška [26] proposed the idea of stabilization of GFEM. First, according to the PUM theorem in the energy norm [24, 25], we give the main approximation result about the relation between global approximation and local approximation. We define the modified local approximation space $\bar{V}_i = \operatorname{span}\{\bar{\varphi}_j^i\}$ associated with $V_i$. Here,

$$\bar{\varphi}_j^i = \varphi_j^i - \pi\varphi_j^i, \quad \text{where } \pi\varphi_j^i := \sum_{k\in\{k(i)|x_{k(i)}\in\omega_i\}} \varphi_j^i(x_k)N_k; \tag{5}$$

$\pi\varphi_j^i$ is the piecewise linear interpolation of $\varphi_j^i$ on the patch $\omega_i$. Clearly, $\bar{\varphi}_j^i = 0$ when $j = 1$. Then the finite-dimensional space $S = S_1 + \bar{S}_2$ is a subspace of $H^1(\Omega)$ with $S_1 = \sum_{i\in I^h} u_i N_i$ and $\bar{S}_2 = \sum_{i\in I} N_i \bar{V}_i$. For the example mentioned $V_i = \mathcal{P}(\omega_i)$, $S_1$ remains unchanged, $\bar{S}_2 = \operatorname{span}\{N_i\bar{\varphi}_2^i, N_i\bar{\varphi}_3^i\}$. The stable XFEM to approximate the solution $u$ of (1) is given by

$$\text{Find } u_h \in S, \text{satisfy } B(u_h, v) = F(v), \quad \forall v \in S. \tag{6}$$

We have the boundary conditions $u|_{\partial\Omega} = 0$ to obtain a unique solution $u_h \in S$. It is called stable XFEM.

Let $a(x, y)$ in (1) be a piecewise constant, we will consider two situations, namely $a(x, y) = a_1$ if $(x, y) \in \Omega_1$ and $a(x, y) = a_2$ if $(x, y) \in \Omega_2$, where the subdomains have the interface: $\Omega_1 \cup \Omega_2 = \Omega$, $\Omega_1 \cap \Omega_2 = \Gamma$.

**Algorithm 3.1**

(i) Suppose that $\Omega$ is a rectangular domain. Find the first-type enriched nodes set $I_1^{\text{en}}$ and elements along interfaces by a level set function. The second-type enriched nodes set $I_2^{\text{en}}$ is chosen by the impact area of intersection. Meanwhile we can easily find the two types of enriched elements.

(ii) The first-type enrichment function $M$ is determined by the level set function $\phi(x)$, here $\phi(x) = 0$, if $x \in \Gamma$ we can use $\phi(x) = -\min_{x_0\in\Gamma} \|x - x_0\|$ as a level set function and discontinuous coefficients across the interfaces.

$$M(x) = \big|\phi(x)\big|. \tag{7}$$

If the function has strong discontinuity, we also need the enrichment function $\operatorname{sign}(\phi)$, so

$$M_1(x) = \operatorname{sign}\big(\phi(x)\big), \qquad M_2(x) = \big|\phi(x)\big|. \tag{8}$$

It is different in standard XFEM, where the enrichment along strong discontinuities is only by $\operatorname{sign}(\phi)$-function.

For the second-type enriched node, we use the four enriched basis functions like SIFs (Stress Intensity Factors) [27]

$$\begin{aligned} &F_1(x) = \sqrt{r}\cos\theta/2, \\ &F_2(x) = \sqrt{r}\sin\theta/2, \\ &F_3(x) = \sqrt{r}\sin\theta\sin\theta/2, \\ &F_4(x) = \sqrt{r}\sin\theta\cos\theta/2. \end{aligned} \tag{9}$$

(iii) Stabilization of the local approximation space. Let $x \in \omega_i$,

$$\begin{aligned} &\overline{M}_j(x) = M_j(x) - I_{\omega_i} M_j(x), \quad j = 1, 2, \\ &\overline{F}_j(x) = F_j(x) - I_{\omega_i}\big(F_j(x)\big), \quad j = 1, 2, 3, 4. \end{aligned} \tag{10}$$

Here $\omega_i$ is the abbreviation of $\omega_i^h$ mentioned above, $I_{\omega_i}(\varphi_j^i)$ is the piecewise linear interpolation of $\varphi_j^i$ on the patch $\omega_i$.

$$I_{\omega_i}\big(\varphi_j^i\big) = \sum_{x_k \in \omega_i} \varphi_j^i(x_k) N_k(x)|_{\omega_i}. \tag{11}$$

(v) Construction element stiff matrix is called EMAT, and the unit load vector is called ERHS. The freedoms associated were increased to six.

$$\begin{aligned} &\psi = [N; \overline{M}; \overline{F}_2; \overline{F}_2; \overline{F}_3; \overline{F}_4], \\ &\mathrm{EMAT}_{i,j} = \int_E a \nabla\psi_i \nabla\psi_j \, dx\, dy, \\ &\mathrm{ERHS}_j = \int_E f\psi_j \, dx\, dy. \end{aligned}$$

Then we can get the whole stiff matrix and solve the finite element equation.

$$\mathrm{EMAT}\vec{\mathbf{x}} = \mathrm{ERHS}. \tag{12}$$

Here, $\mathbf{x}$ is the vector that equals $\mathbf{x} = (\vec{u}, \vec{u}^{\mathrm{en}})$.

(vi) Output the numerical result and error.

**Remark 3.1** The element stiff matrix size varies with different types of elements. The common element far away from interfaces has four freedoms, while the element near intersection has 24 degrees of freedoms.

**Remark 3.2** When computing the integration on the element containing intersection, we decompose the element into several triangles by the location of intersection.

The XFEM is a PUM, where

(1) the patches $\omega_i^h$ are 'FE stars' relative to a finite element (FE) rectangulation of $\Omega$;

(2) the piecewise linear FE hat function $N_i$ associated with the vertices of FE rectangularity serves as the PU.

Supposing $u \in H_0^1(\Omega)$ is the solution of (1), we use Q1-element as the PU function.

Next we discuss the semi-definiteness of the stiff matrix of the stable XFEM. From the definition of $V$, any $v \in V$ has the following:

$$v(x) = \sum_{i\in I} u_i N_i(x) + \sum_{i\in I}\sum_{j=1}^{5} b_{ij} N_i(x)\psi_j(x); \quad u_i, b_{ij} \in \mathbb{R},$$

where $\psi_j(x)$ is $\overline{M}(x)$, $\overline{F}_l(x)$, $l = 1,2,3,4$. For each element, we can get the single stiff matrix, $B(v_i, v_j) = \int_\Omega a\nabla v_i \cdot \nabla v_j \, dx\, dy$. The value can be divided into three types as follows:

(1) If $v_i \in S_1$, $v_j \in S_1$, $B_{ij} = B(N_i, N_j)$, which is the basic part of XFEM, is the standard $N \times N$ FE stiffness matrix.

(2) If $v_i \in S_1$, $v_j \in S_2$ or $v_i \in S_2$, $v_j \in S_1$, $B_{ij} = 0$ and $B_{ji} = 0$, because the $S_1$ and $S_2$ are orthogonal in the inner product $B(\cdot,\cdot)$.

(3) If $v_i \in S_2$, $v_j \in S_2$, $B_{ij} = B(N_i\psi^i, N_j\psi^j)$, $B_{22}$ is only associated with some vertices $x_i(j) \in I_1^{\mathrm{en}}$ or $I_2^{\mathrm{en}}$. The additional degrees of freedom are introduced here. We can get the stiff matrix

$$A = \begin{pmatrix} K_U & K_{UA} \\ K_{AU} & K_A \end{pmatrix}.$$

It is well known that the standard FE stiffness matrix block is block-tridiagonal, and we can get the argument that the matrix block $K_U$ is positive definite. If the matrix block $K_A$ is also positive definite, the stiff matrix $A$ of the stable XFEM will be positive definite.

### 3.2 The analysis of stable XFEM

**Theorem 3.1** *Let $u \in H^1(\omega_i)$. Suppose that for $i \in I^h$, there exist $\varsigma^i \in V_i$ and $C^1 > 0$, independent of $i$, such that*

$$\|u - \varsigma_i\|_{L^2(\omega_i)} \le C_1 \operatorname{diam}(\omega_i)\|u - \varsigma_i\|_{\varepsilon(\omega_i)} \quad \textit{and} \quad \|u - \varsigma_i\|_{\varepsilon(\omega_i)} \le \epsilon_i.$$

*Then there exists $v \in V$ such that*

$$\|u - u_h\|_{\varepsilon(\Omega)} \le \inf_{v\in V} \|u - v\|_{\varepsilon(\Omega)} \le C\left(\sum_{i\in I^h} \epsilon_i^2\right)^{1/2},$$

*where the positive constant $C$ depends on $\kappa$, $C_1$, $\frac{\alpha}{\beta}$* [24, 25].

It is easy to check that the argument in Theorem 3.1 holds. Actually, there exists $\xi_i \in V_i$ such that $\|u - \xi_i\|_{\varepsilon(\omega_i)} \le Ch|u|_{H^1(\omega_i)}$, $\|u - \xi_i\|_{L^2(\omega_i)} \le Ch^2|u|_{L^2(\omega_i)}$, then we can get

$$\begin{aligned} &\|u - u_h\|_{L^2(\Omega)} = \mathcal{O}\big(h^2\big), \\ &\|u - u_h\|_{\varepsilon(\Omega)} = \mathcal{O}(h), \end{aligned} \tag{13}$$

where $u_h$ is the solution of the stable extended finite element method (SXFEM).

**Theorem 3.2** *Let $u \in H^1(\Omega)$ be the solution of* (1). *Suppose that for each $x_i$, which is in the enriched node set, there exist $\bar{\xi}^i \in \bar{V}_i$ and $C_0 > 0$, which are independent of i, such that*

$$\begin{aligned} &\|u - \pi_{\omega_i} u - \bar{\xi}\|_{L^2(\omega_i)} \le C_0 \operatorname{diam}(\omega_i) \left\|u - \pi_{\omega_i} u - \bar{\xi}^i\right\|_{\varepsilon(\omega_i)}, \\ &\|u - \pi_{\omega_i} u - \bar{\xi}\|_{\varepsilon(\omega_i)} \le \epsilon_{1i}. \end{aligned} \tag{14}$$

*Then there exists $v \in S = S_1 + \bar{S}_2$ such that*

$$\begin{aligned} &\|u - v\|_{\varepsilon(\Omega)} \le C \left( \sum_{x_i \in I} \|u - \pi_{\omega_i} u\|^2_{\varepsilon(\omega_i)} + \sum_{x_i \in I_2} \epsilon_i^2 \right)^{1/2}, \\ &\|u - v\|_{L^2(\Omega)} \le C_1 \left( \sum_{x_i \in I} \|u - \pi_{\omega_i} u\|^2_{L^2(\omega_i)} + \sum_{x_i \in I^{\mathrm{en}}} \epsilon_i^2 \right)^{1/2}. \end{aligned} \tag{15}$$

*Proof* Define $w := u - \pi_h u$, and let $\bar{v} := \sum_{x_i \in I^{\mathrm{en}}} N_i \bar{\xi}^i \in \bar{S}_2$. $\{N_i\}_{x_i \in I}$, using a bilinear quadrangle element (Q1) as a PU,

$$w - \bar{v} = \sum_{x_i \in I} N_i w - \sum_{x_i \in I^{\mathrm{en}}} N_i \bar{\xi}^i = \sum_{x_i \in I \setminus I^{\mathrm{en}}} N_i w - \sum_{x_i \in I^{\mathrm{en}}} N_i \left(w - \bar{\xi}^i\right).$$

So

$$\|w - \bar{v}\|^2_{\varepsilon(\Omega)} \le C \left( \left\| \sum_{x_i \in I \setminus I^{\mathrm{en}}} N_i w \right\|^2_{\varepsilon(\Omega)} + \left\| \sum_{x_i \in I^{\mathrm{en}}} N_i \left(w - \bar{\xi}^i\right) \right\|^2_{\varepsilon(\Omega)} \right). \tag{16}$$

We address the second term of (16) on the right, for any $x \in \Omega$, it is at most four patches. So the sum $\sum_{x_i \in I^{\mathrm{en}}} \nabla(N_i(w - \bar{\xi}))$ has at most four terms for any $x \in \Omega$. If we use uniform grids for the whole domain, $\|N_i'\|_{L^\infty} \le C_0(\operatorname{diam}\{w_i\})^{-1} = C_0 \frac{1}{h}$, and using (14), we can show that

$$\begin{aligned} &\left\| \sum_{x_i \in I^{\mathrm{en}}} N_i \left(w - \bar{\xi}^i\right) \right\|^2_{\varepsilon(\Omega)} \\ &\quad = \int_{\Omega^{\mathrm{en}}} a \left| \nabla(N_i) \left(w - \bar{\xi}^i\right) + N_i \left(\nabla \left(w - \bar{\xi}^i\right)\right) \right|^2 dx\, dy \\ &\quad \le 2 \int_{\Omega^{\mathrm{en}}} \left( \sum_{x_i \in I^{\mathrm{en}}} a \nabla(N_i) \left(w - \bar{\xi}^i\right) \right)^2 dx\, dy + 2 \int_{\Omega^{\mathrm{en}}} \left( \sum_{x_i \in I^{\mathrm{en}}} a N_i \nabla \left(w - \bar{\xi}^i\right) \right)^2 dx\, dy \\ &\quad \le 8 \int_{\omega_i} a \sum_{x_i \in I^{\mathrm{en}}} \left( \nabla(N_i) \left(w - \bar{\xi}^i\right) \right)^2 dx\, dy + 8 \int_{\omega_i} a \sum_{x_i \in I^{\mathrm{en}}} \left( N_i \nabla \left(w - \bar{\xi}^i\right) \right)^2 dx\, dy \\ &\quad \le 8k \left( c \sum_{x_i \in I^{\mathrm{en}}} \frac{\epsilon_{0j}^2}{h} + \sum_{x_i \in I^{\mathrm{en}}} \left\| w - \bar{\xi}^i \right\|^2_{\varepsilon(\omega_i)} \right) \\ &\quad \le C \sum_{x_i \in I^{\mathrm{en}}} \left\| w - \bar{\xi}^i \right\|^2_{\varepsilon(\omega_i)} \le \sum_{x_i \in I^{\mathrm{en}}} \epsilon_{1i}^2. \end{aligned} \tag{17}$$

With the similar argument and the interpolation estimate, we have

$$\|w\|_{L^2(\omega_i)} = \|u - \pi_{\omega_i}\|_{L^2(\omega_i)} \le Ch \|u - \pi_{\omega_i}\|_{\varepsilon(\omega_i)}.$$

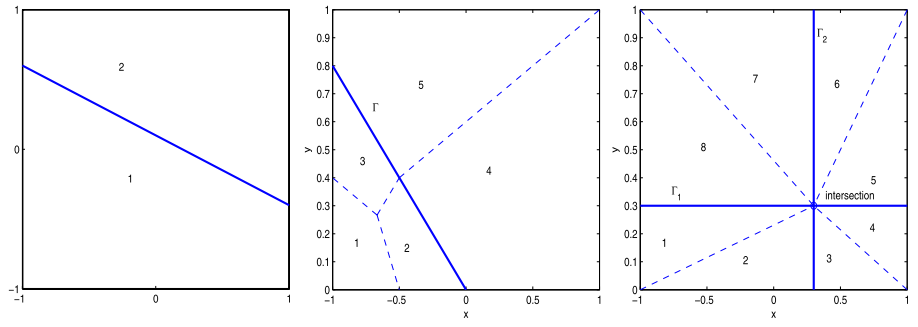


**Figure 1 Dividing a fully or partially cut element into subelements, left: 2, middle: 5, right: 8.**

Then we get the first term on the right-hand side of (16)

$$\Big\| \sum_{x_i \in I \setminus I^{\mathrm{en}}} N_i w \Big\|^2_{\varepsilon(\Omega)} \leq C \sum_{x_i \in I \setminus I^{\mathrm{en}}} \|u - \pi_{\omega_i}\|^2_{\varepsilon(\Omega)}.$$

Finally, according to (14), we have

$$\|w - \bar{\nu}\|^2_{\varepsilon(\Omega)} = \|u - \pi_h u - \bar{\nu}\|^2_{\varepsilon(\Omega)} \leq C\Big( \sum_{x_i \in I \setminus I^{\mathrm{en}}} \|u - \pi_{\omega_i} u\|^2_{\varepsilon(\omega_i)} + \sum_{x_i \in I^{\mathrm{en}}} \epsilon^2_{1i} \Big)$$

by setting $\nu = \pi_h u + \bar{\nu} \in S_1 + \bar{S_2}$. □

## 4 Modified numerical integration for XFEM

*In standard FEM, we often use standard Gauss integration in all elements because the shape functions are smooth in the inner of the element. However, if the problem has interface, the smoothness could not be guaranteed in some elements cut by an interface. In XFEM* [28], *give the outline of integration strategy.*

In this work we first divide the special element into subelements as shown in Figure 1. We can find that the subelements may contain a triangle, a common quadrangle or curved edge graphics, especially if the element contains intersection of interfaces shown in the right figure of Figure 1. We should utilize the vertices of element, the intersection of the edge and interface, the intersection of different interfaces. In order to get more accurate integration, the subdivision uses the same number of Gauss nodes with other regular element.

This numerical integration strategy is also suitable for both extrinsic and intrinsic XFEM. If the interface Γ is curve, from Figure 2 we should first approximate it by several segments of bounding polygon and use more subdivisions in Figure 1. Of course we can use more segments in order to approximate the curve of interface.

## 5 Numerical test

We use Matlab to implement our methods. First we introduce some notations. nElem = $\mathrm{nElem}_x$ = $\mathrm{nElem}_y$ means we have uniform meshes in $x$-direction and $y$-direction $h$ = 2/nElem,

SFEM means the standard finite element method,

SXFEM means the stable extended finite element method,

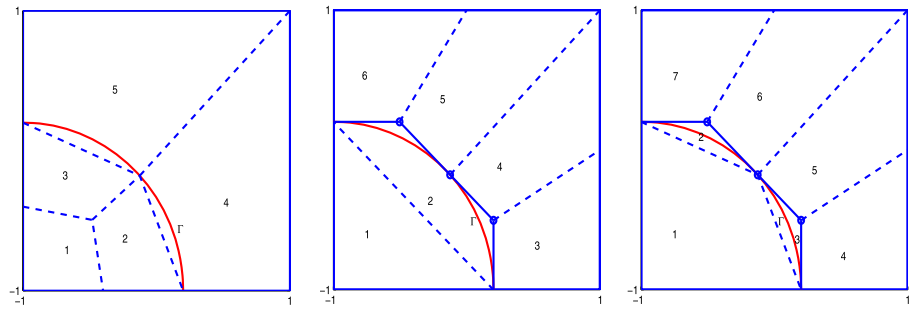

**Figure 2 Dividing a fully or partially cut element into subelements, left: 2, middle: 5, right: 8.**

DOF means the degrees of freedom,

$\|u-u_h\|_0$: the relative $L_2$-error for $u_h$ using SXFEM,

$\text{order}_{L_2}$ means the convergence rate in $L_2$-error order,

$\|u-u_h\|_E$: the relative energy-error for $u_h$ using SXFEM, we get the result by

$$\|u-u_h\|_E = \left(\int_\Omega a(x,y)\big(\nabla(u-u_h)\big)^2\,dx\,dy\right)^{1/2} \Big/ \left(\int_\Omega a(x,y)(\nabla u)^2\,dx\,dy\right)^{1/2},$$

$\text{order}_E$ means the convergence rate in energy-norm.

In this section we choose the standard benchmark test and report some numerical results for an interface problem with intersecting interfaces used by many researchers, see [1, 29, 30]. Let $\Omega = (-1,1)\times(-1,1)$, the exact solution is as follows:

$$u(r,\theta) = r^\beta \mu(\theta)$$

in polar coordinates at the origin with

$$\mu(\theta) = \begin{cases} \cos(\beta(\frac{\pi}{2}-\sigma))\cos(\beta(\theta-\frac{\pi}{2}+\rho)) & \text{if } \theta\in[0,\frac{\pi}{2}],\\ \cos(\beta\rho)\cos(\beta(\theta-\pi+\sigma)) & \text{if } \theta\in[\frac{\pi}{2},\pi],\\ \cos(\beta\sigma)\cos(\beta(\theta-\pi-\rho)) & \text{if } \theta\in[\pi,\frac{3\pi}{2}],\\ \cos(\beta(\frac{\pi}{2}-\rho))\cos(\beta(\theta-\frac{3\pi}{2}-\sigma)) & \text{if } \theta\in[\frac{3\pi}{2},2\pi], \end{cases}$$

where $\rho$, $\sigma$ are constant numbers. The exact solution satisfies (1), $f=0$ and $a(x,y)=R$ if $(x,y)\in(0,1)^2\cup(-1,0)^2$, and $a(x,y)=1$ if $(x,y)\in\Omega\backslash([0,1]^2\cup[-1,0]^2)$. The numbers $\beta$, $R$, $\sigma$ and $\rho$ satisfy nonlinear relations (*e.g.*, [29, 30])

$$R\approx 161.4476387975881,\qquad \rho=\pi/4\quad\text{and}\quad \sigma\approx 14.92256510455152.$$

Here, $\beta=0.1$, it is a difficult problem for computation by standard FEM. The exact solution is singular on the origin node and the interfaces $\Gamma$ are $x$-axis and $y$-axis (fixed by the discontinuity of $a(x,y)$). $\Gamma_1:(x,y)|xy=0,x\geq 0$, $\Gamma_2:(x,y)|xy=0,y\geq 0$, $\Gamma_3:(x,y)|xy=0,x\leq 0$ and $\Gamma_4:(x,y)|xy=0,y\leq 0$ The origin node $(0,0)$ is the intersecting interfaces.

In this test we use Q1 element, all nodes are divided into three different types as follows:

1. The node with influence area $\omega(x_i)\cap\Gamma_i=\emptyset$;
2. The node with influence area $\omega(x_i)$, singularity node $O$, $O\in\omega(x_i)$;

**Table 1 DOF, the energy-error and L2-error using sXFEM for different step, impact radius $r = 0.1$**

| $2/h$ | DOF | $\|u - u_h\|_0$ | $\text{order}_{L2}$ | $\|u - u_h\|_E$ | $\text{order}_E$ |
|---|---|---|---|---|---|
| 19 | 416 | $3.14410816 \times 10^{-4}$ | \ | $2.88823845 \times 10^{-2}$ | \ |
| 39 | 1648 | $1.31537498 \times 10^{-4}$ | 2.1536 | $1.36757789 \times 10^{-2}$ | 1.0785 |
| 79 | 6608 | $3.14410816 \times 10^{-5}$ | 2.0647 | $6.66191594 \times 10^{-3}$ | 1.0376 |
| 159 | 26432 | $8.09627168 \times 10^{-6}$ | 1.9573 | $3.28872649 \times 10^{-3}$ | 1.0184 |

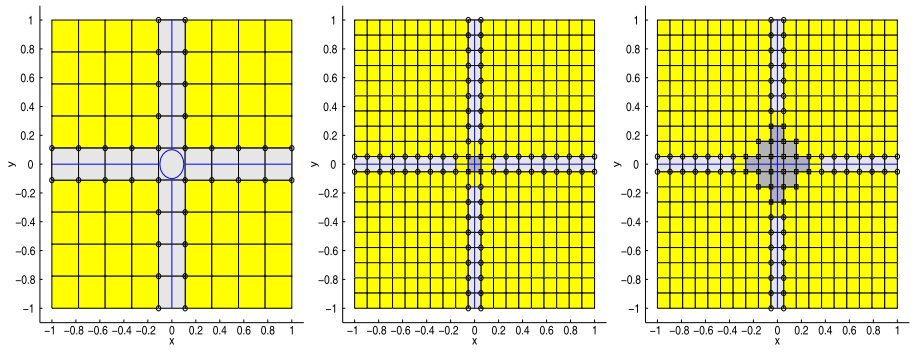

**Figure 3 The mesh and interface and intersection nodes and area: left, $r = 0.1$, $h = 2/11$, middle $r = 0.1$, $h = 2/19$ and right $r = 0.3$, $h = 2/19$.**

3. Other elements. Not all the nodes in these elements need to be enriched(one, two or three nodes are enriched in some elements).

We talk about the 2nd-enriched nodes chosen. Table 1 shows that the error does decrease dramatically when the impact area increases, so we can choose the impact area radius $r = 0.1$ or $r = \sqrt{2}h$. We just need guarantee that at least there is an element that is enriched (all nodes of the element are enrichment nodes). For example, in Figure 3 we can choose the gray color circle area, not the left of Figure 3 ($r = h$ it is considered as the 1st enriched nodes). Table 2 also verifies that the impact radius is not important for the development of error.

We list the numerical error by stable XFEM and DOF when the impact radius is $r = 0.1$ in Table 1. We can easily find that our method has reached the optimal orders. In Table 2 we also list the numerical error with different impact radius, the error is not decreased when the radius is larger. Generally $r = \sqrt{2}h$ is enough. In the last Table 3, we show the L2-error by FEM and XFEM and stable extrinsic XFEM with the same mesh. It is shown that the FEM only has a half of order of optimal convergence. And the intrinsic XFEM is a little better than stable XFEM.

For two types of XFEM, the L2-error is $o(h^2)$, and the energy-error is $o(h)$. It is better than that of FEM, we do not list the result of the reference [1] using a triangular element. According to Figure 4, it is shown that difference of the error distribution about FEM method and sXFEM. The result in their reference the absolute energy-error is often considered to be 0.05, while the degree of freedom is about 3,475. According to the results of our method numerical relative energy-error is $1.36757789 \times 10^{-2}$, while DOF number is only 1,648. If we use the variable step size, we will get more efficient result. We take the further work into consideration.

**Table 2 DOF, the energy-error and L2-error using sXFEM with different impact radius *r***

| 2/*h* | *r* | DOF | $\|u - u_h\|_0$ | $\|u - u_h\|_E$ |
|---|---|---|---|---|
| 51 | 0.05 | 2720 | $7.62956091 \times 10^{-5}$ | $1.03929952 \times 10^{-2}$ |
| 51 | 0.1 | 2800 | $7.63216118 \times 10^{-5}$ | $1.03929961 \times 10^{-2}$ |
| 51 | 0.2 | 3024 | $7.64345134 \times 10^{-5}$ | $1.03929957 \times 10^{-2}$ |
| 51 | 0.3 | 3456 | $8.01596131 \times 10^{-5}$ | $1.03930097 \times 10^{-2}$ |

**Table 3 Comparison of L2-error ($\|u - u_h\|_0$) using standard FEM, stable XFEM and modified intrinsic XFEM**

| 2/*h* | FEM | XFEM | SXFEM |
|---|---|---|---|
| 19 | $1.29367331 \times 10^{-2}$ | $5.85229689 \times 10^{-4}$ | $5.97809622 \times 10^{-4}$ |
| 39 | $6.11857595 \times 10^{-3}$ | $1.31518929 \times 10^{-4}$ | $1.55184343 \times 10^{-4}$ |
| 79 | $2.97964019 \times 10^{-3}$ | $3.12260721 \times 10^{-5}$ | $3.14410816 \times 10^{-5}$ |
| 159 | $1.47079316 \times 10^{-3}$ | $7.61075872 \times 10^{-6}$ | $8.09627168 \times 10^{-6}$ |
| 319 | $7.30756777 \times 10^{-4}$ | $1.87886932 \times 10^{-6}$ | $2.47196080 \times 10^{-6}$ |

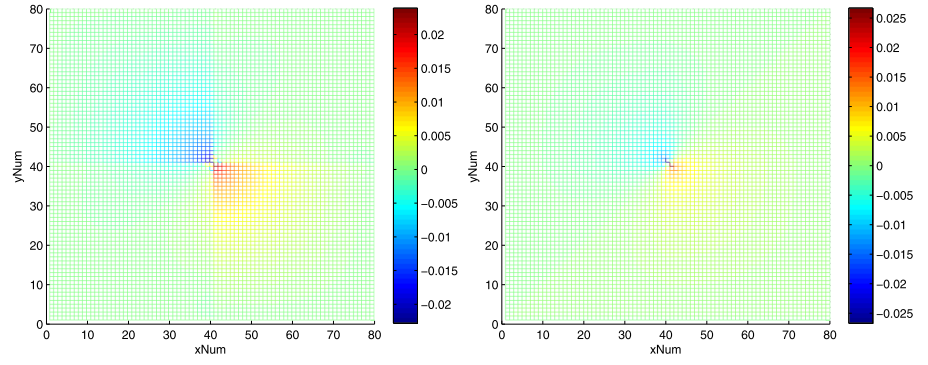


**Figure 4 Error distribution by different methods: standard FEM, stable XFEM ($h = 2/79$).**

## 6 Conclusions

In this article, we discussed the stable XFEM for the second order elliptic equation with discontinuous coefficients and derivative of solutions, and it comes to the following conclusions. Firstly we modified the local enrichment function space, and we analyzed how the global error can be dominated by the local error. It was different from the shift function only changed in vertices [31]. Secondly we described the stable XFEM step by step, we also gave the error estimation if we use Q-1 element. The L2-error is $o(h^2)$, and energy-error is $o(h)$. We also got the optimal convergence same with SXFEM. Two types of XFEM are better than FEM, to adapt the FEM result in reference [1] a triangular element was used. There the absolute energy-error was considered as 0.05, while the DOF is about 3,475. Numerical relative energy-error in this paper was $1.36757789 \times 10^{-2}$, while DOF is only 1,648. We will extend our method in general area, and it can be used to different meshes and high order polynomials. At last we gave the numerical simulation for the standard benchmark example. Numerical results support our analysis, we get the optimal order for energy-error and L2-error, respectively.

**Competing interests**
The authors declare that they have no competing interests.

**Authors' contributions**
All authors contributed equally to the writing of this paper. All authors read and approved the final manuscript.

**Author details**
[1]College of Mathematics and System Sciences, Xinjiang University, Urumqi, 830046, China. [2]Cele National Station of Observation and Research for Desert-Grassland Ecosystem, Xinjiang Institute of Ecology and Geography, Urumqi, 830011, China. [3]School of Mathematics and Statistics, Xi'an Jiaotong University, Xi'an, 710049, China. [4]School of Mathematics Science, Qingdao University, Qingdao, 266071, China.

**Acknowledgements**
The authors of this work are grateful to the journal editors and the anonymous reviewers for their comments and recommendations, which have greatly improved our manuscript and made it more suitable for readers of the journal. This work is subsidized by China Postdoctoral Science Foundation funded project (No. 2014M562487) and NSFC of China (Nos. 11461068, 11171269, 11401332, 61163027, 11362021).

Received: 28 November 2014 Accepted: 25 May 2015 Published online: 15 July 2015

**References**

1. Cai, ZQ, Zhang, S: Recovery-based error estimator for interface problems: conforming linear elements. SIAM J. Numer. Anal. **47**, 2132-2156 (2009)
2. Bernardi, C, Verfürth, R: Adaptive finite element methods for elliptic equations with non-smooth coefficients. Numer. Math. **85**, 579-608 (2000)
3. Peskin, CS: Numerical analysis of blood flow in heart. J. Comput. Phys. **25**, 220-252 (1977)
4. Leveque, RJ, Li, ZL: The immersed interface method for elliptic equations with discontinuous coefficients and singular sources. SIAM J. Numer. Anal. **31**, 1019-1044 (1994)
5. Fogelson, AL, Keener, JP: Immersed interface methods for Neumann and related problems in two and three dimensions. SIAM J. Sci. Comput. **22**, 1630-1684 (2000)
6. Li, Z, Ito, K, Lai, M-C: An augmented approach for Stokes equations with a discontinuous viscosity and singular forces. Comput. Fluids **36**, 622-635 (2007)
7. Huang, H, Li, Z: Convergence analysis of the immersed interface method. IMA J. Numer. Anal. **19**, 583-608 (1999)
8. Wiegmann, A, Bube, KP: The explicit-jump immersed interface method: finite difference methods for PDEs with piecewise smooth solutions. SIAM J. Numer. Anal. **37**(3), 827-862 (2000)
9. Berthelsen, PA: A decomposed immersed interface method for variable coefficient elliptic equations with non-smooth and discontinuous solutions. J. Comput. Phys. **197**, 364-386 (2004)
10. Zhao, JP, Hou, YR, Li, YF: Immersed interface method for elliptic equations based on a piecewise second order polynomial. Comput. Math. Appl. **63**, 957-965 (2012)
11. Xia, KL, Zhan, M, Wei, G-W: The matched interface and boundary (MIB) method for multi-domain elliptic interface problems. J. Comput. Phys. **230**, 8231-8258 (2011)
12. Zhou, YC, Zhao, S, Feig, M, Wei, GW: High order matched interface and boundary method for elliptic equations with discontinuous coefficients and singular sources. J. Comput. Phys. **213**, 1-30 (2006)
13. Pan, KJ, Tan, YJ, Hu, HL: An interpolation matched interface and boundary method for elliptic interface problems. J. Comput. Appl. Math. **234**, 73-94 (2010)
14. Li, Z: The immersed interface method using a finite element formulation. Appl. Numer. Math. **27**, 253-267 (1998)
15. Xie, H, Li, Z, Qiao, Z: A finite element method for elasticity interface problems with locally modified triangulations. Int. J. Numer. Anal. Model. **8**, 189-200 (2011)
16. Lin, T, Lin, Y, Zhang, X: A method of lines based on immersed finite elements for parabolic moving interface problems. Adv. Appl. Math. Mech. **5**(4), 548-568 (2013)
17. Lin, T, Sheen, D: The immersed finite element method for parabolic problems with the Laplace transformation in time discretization. Int. J. Numer. Anal. Model. **10**(2), 298-313 (2013)
18. He, XM, Lin, T, Lin, YP: Immersed finite element methods for elliptic interface problems with non-homogeneous jump conditions. Int. J. Numer. Anal. Model. **8**, 284-301 (2011)
19. Belytschko, T, Black, T: Elastic crack growth in finite elements with minimal remeshing. Int. J. Numer. Methods Eng. **45**, 601-620 (1999)
20. Moës, N, Dolbow, J, Belytschko, T: A finite element method for crack growth without remeshing. Int. J. Numer. Methods Eng. **46**, 131-150 (1999)
21. Sukumar, N, Chopp, DL, Moës, N, Belytschko, T: Modeling holes and inclusions by level sets in the extended finite-element method. Comput. Methods Appl. Mech. Eng. **190**, 6183-6200 (2001)
22. Chessa, J, Wang, H, Belytschko, T: On the construction of blending elements for local partition of unity enriched finite elements. Int. J. Numer. Methods Eng. **57**, 1015-1038 (2003)
23. Wu, JY: Unified analysis of enriched finite elements for modeling cohesive cracks. Comput. Methods Appl. Mech. Eng. **200**, 3031-3051 (2011)
24. Babuška, I, Melenk, JM: The partition of unity method. Int. J. Numer. Methods Eng. **40**, 727-758 (1997)
25. Melenk, JM, Babuška, I: The partition of unity finite element method: basic theory and application. Comput. Methods Appl. Mech. Eng. **139**, 289-314 (1997)
26. Babuška, I, Banerjee, U: Stable generalized finite element method (SGFEM). Comput. Methods Appl. Mech. Eng. **201**, 91-111 (2012)
27. Liu, XY, Xiao, QZ, Karihaloo, BL: XFEM for direct evaluation of mixed mode SIFs in homogeneous and bi-materials. Int. J. Numer. Methods Eng. **59**, 1103-1118 (2004)
28. Fries, TP, Belytschko, T: The intrinsic XFEM: a method for arbitrary discontinuities without additional unknowns. Int. J. Numer. Methods Eng. **68**, 1358-1385 (2006)
29. Kellogg, RB: On the Poisson equation with intersecting interfaces. Appl. Anal. **4**, 101-129 (1975)
30. Morin, P, Nochetto, RH, Siebert, KG: Convergence of adaptive finite element methods. SIAM Rev. **44**, 631-658 (2002)
31. Fries, TP, Belytschko, T: The extended-generalized finite element method: an overview of the method and its applications. Int. J. Numer. Methods Eng. **84**, 253-304 (2010)